31. N. H. Sleep, K. Zahnle, *J. Geophys. Res.* **103**, 28529 (1998).
32. S. J. Mojzsis, T. M. Harrison, *GSA Today* **10**, 1 (April 2000).
33. N. H. Sleep, K. J. Zahnle, J. F. Kasting, H. J. Morowitz, *Nature* **342**, 139 (1989).
34. E. Pierazzo, C. F. Chyba, *Meteorit. Planet. Sci.* **34**, 909 (1999).
35. D. A. Kring, *GSA Today* **10**, 1 (August 2000).
36. P. R. Renne *et al.*, *Chem. Geol.* **145**, 117 (1998).
37. C. M. Hohenberg, K. Marti, F. A. Podosek, R. C. Reedy, J. R. Shirck, *Proc. Lunar Planet. Sci. Conf.* **9**, 2311 (1978).
38. T. D. Swindle, in *Meteorites and the Early Solar System* J. F. Kerridge, M. S. Matthews, Eds. (Univ. of Arizona Press, Tucson, 1988), pp. 535–564.
39. B. A. Cohen, thesis, University of Arizona (2000).
40. We thank A. Bischoff and J. Zipfel for providing us with DaG 262 and DaG 400. L. Dones and an anonymous reviewer provided constructive reviews. This research was supported with a NASA Space Grant Fellowship (B.A.C.) and by NAG5-4944 (D.A.K.) and NAG5-4767 (T.D.S.) and used the NASA Astrophysical Data System Abstract Service.

22 August 2000; accepted 20 October 2000

Nitric Acid Trihydrate (NAT) in Polar Stratospheric Clouds

Christiane Voigt,[1] Jochen Schreiner,[1] Andreas Kohlmann,[1] Peter Zink,[1] Konrad Mauersberger,[1]* Niels Larsen,[2] Terry Deshler,[3] Chris Kröger,[3] Jim Rosen,[3] Alberto Adriani,[4] Francesco Cairo,[4] Guido Di Donfrancesco,[4] Maurizio Viterbini,[4] Joelle Ovarlez,[5] Henri Ovarlez,[5] Christine David,[6] Andreas Dörnbrack[7]

A comprehensive investigation of polar stratospheric clouds was performed on 25 January 2000 with instruments onboard a balloon gondola flown from Kiruna, Sweden. Cloud layers were repeatedly encountered at altitudes between 20 and 24 kilometers over a wide range of atmospheric temperatures (185 to 197 kelvin). Particle composition analysis showed that a large fraction of the cloud layers was composed of nitric acid trihydrate (NAT) particles, containing water and nitric acid at a molar ratio of 3:1; this confirmed that these long-sought solid crystals exist well above ice formation temperatures. The presence of NAT particles enhances the potential for chlorine activation with subsequent ozone destruction in polar regions, particularly in early and late winter.

Since the early 1980s, the formation of a large ozone hole above Antarctica during southern spring has become a yearly event. Stratospheric air isolated within the polar vortex cools during winter to temperatures that allow the formation of polar stratospheric clouds (PSCs) at altitudes between 15 and 25 km (*1*). The cloud particles provide surfaces for the activation of otherwise relatively unreactive chlorine-containing molecules. Upon the return of sunlight in the spring, the cloud-processed chlorine species are photolyzed and induce dramatic ozone losses (*2*). To a lesser extent, the north polar stratosphere also experiences low winter temperatures within a well-developed vortex, leading to the formation of PSCs and subsequent ozone destruction (*3*). Satellite and field measurements in both polar regions have shown that many PSCs exist well above the frost point of water, T_{ICE}, the temperature in the stratosphere near 188 K below which ice particles can form (*4–6*). For those PSCs the important role of the trace gas nitric acid (HNO_3) has been recognized. Early atmospheric models predicted the formation of solid nitric acid hydrate crystals at temperatures above T_{ICE} (*7, 8*). Laboratory studies revealed that nitric acid trihydrate (NAT, $HNO_3 \cdot 3H_2O$) would be stable up to 7° above the frost point in the lower stratosphere (*9*). Measurements at these temperatures from high-flying aircraft and ground-based LIDAR (light detection and ranging), however, often identified liquid supercooled ternary solution (STS) droplets instead of solid particles (*10–12*).

The composition, phase, and formation temperature range of PSCs are critical for atmospheric models that predict ozone losses in polar regions. NAT is believed to be the most stable particle under stratospheric conditions. As a result of its low vapor pressure, NAT can exist at higher temperatures than STS droplets or ice particles, with the consequence that chlorine activation can proceed over wider areas and for longer time periods. By scavenging nitrogen compounds, NAT particles hinder the passivation of active chlorinated substances through reactions with nitrogen oxides. The removal of particles through sedimentation to lower altitudes, a process called denitrification, increases the efficiency of chlorine activation and is only possible through the formation of crystalline PSC particles. Despite their importance, no direct chemical analysis of NAT particles in the stratosphere has been made, although they have been identified in many laboratory studies (*9, 13*) and inferred from atmospheric measurements (*6*).

In January 1998, a direct particle composition measurement was performed in lee wave–induced PSCs above Scandinavia (*14–16*). STS droplets containing water, nitric acid, and sulfuric acid were observed. As expected from STS theory, a close correlation between low atmospheric temperatures and the presence of PSCs was found. A more comprehensive set of instruments to investigate chemical, physical, and optical properties of PSCs was launched at 20 UT (universal time) on 25 January 2000 from the balloon facility Esrange, near Kiruna, Sweden. The crucial instrument on both flights was an aerosol composition mass spectrometer (ACMS) that uses an aerodynamic lens to focus particles into a narrow beam (*17*) and separates them from ambient gases. The particles are then evaporated inside a small sphere, and the evolving gases are analyzed with a mass spectrometer. Simultaneous measurements of particle number density and size were performed with particle counters (*18, 19*). Backscatter ratios and depolarization were measured with two backscatter sondes (*20, 21*). A water vapor experiment determined the frost point T_{ICE} (*22*). A number of sensors measured the ambient stratospheric temperature with a precision better than ±0.5 K to establish a correlation with PSC particle parameters such as volume and composition.

A vertical cross section of the temperature distribution along the flight track at 22 UT was simulated with a mesoscale meteorological model (*23*) (Fig. 1). The balloon trajectory (thick line) crosses the extension of a cold trough that had developed over the Scandinavian mountains as a result of adiabatic expansion of ascending air masses in mountain-induced gravity waves. Temperatures determined during the flight are in general agreement with the model simulations, although the latter cannot resolve the measured small-scale temperature fluctuations. The cold temperature pattern between 21 and 24 km extended upwind toward the Scandinavian mountains, indicating that particles sampled during the flight could have nucleated in those cold regions. Near 22 km on the first ascent, the observed temperatures were 1 to 2 K below T_{ICE}. During the 2-hour mea-

[1]Max-Planck-Institut für Kernphysik, Division of Atmospheric Physics, Post Office Box 103 980, D-69029 Heidelberg, Germany. [2]Division of Middle Atmosphere Research, Danish Meteorological Institute, Lyngbyvej 100, DK-2100 Copenhagen, Denmark. [3]Department of Atmospheric Science, University of Wyoming, Post Office Box 3038, Laramie, WY 82071, USA. [4]CNR-Istituto di Fisica dell'Atmosfera, Via Fosso del Cavaliere 100, I-00133 Rome, Italy. [5]Laboratoire de Météorologie Dynamique du CNRS, École Polytechnique, F-91128 Palaiseau, France. [6]Service d'Aéronomie du CNRS, Institut Pierre-Simon Laplace, Université Paris, 4 place Jussieu, F-75252 Paris, France. [7]DLR Oberpfaffenhofen, Institut für Physik der Atmosphäre, D-82234 Wessling, Germany.

*To whom correspondence should be addressed. E-mail: Konrad.Mauersberger@mpi-hd.mpg.de

surement period, flight operators were able to raise and lower the balloon repeatedly to sample cloud layers between 21 and 24 km.

A layer of particles with median diameters of 1 to 2 μm and concentrations of less than 0.5 particles/cm^3 was penetrated at 75,700, 77,500, 79,700, and 81,000 s UT (Fig. 2). In these layers, strong fluctuations in the condensed water and nitric acid signal result from low–particle number counting statistics. The condensed water data demonstrate that single particles can be resolved individually, particularly between 77,600 and 78,300 s UT. Other nitric acid and water measurements do not show such a strong variation in the count rates. Around 75,000, 76,000, and particularly near 77,000 s UT, the water signal distribution shows little fluctuations, the result of the detection of high concentrations (about 15 particles/cm^3) of small particles with a median diameter of 0.1 to 0.5 μm. As opposed to the January 1998 flight (*14*), there is not a close correlation between low temperatures and the presence of clouds.

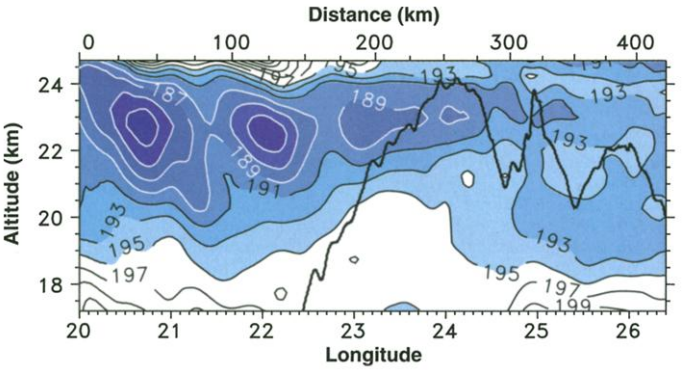

Fig. 1. Simulated temperatures (kelvin) during the balloon flight on 25 January 2000 at 22 UT, using the mesoscale MM5 model (*23*). The mesoscale simulation with 2.6 km horizontal grid size, initialized on 25 January 2000 at 6 UT, was forced by global analysis at 0.5° × 0.5° resolution by the European Center for Medium Range Weather Forecast (ECMWF). The balloon trajectory shows the ascents and descents during the 2-hour time period when measurements were taken, which started and ended at 20-km altitude. The air parcels encountered by the balloon had previously experienced very low temperatures above the Scandinavian mountains. The balloon launch was near Kiruna at 21.1° longitude.

Laboratory calibrations for H_2O and HNO_3 were used to convert the count rates into particle molar ratios of H_2O:HNO_3 (*24*). Signals were integrated over long time scales in distinct cloud layers to minimize the statistical error (Fig. 3) (*25*). Most of the cloud data have a ratio of 3 ± 0.5, identifying NAT particles. In these clouds, particle volumes of 1 to 3 μm^3/cm^3 were measured, which to a large extent agree with model calculations of NAT particle volumes (*12*). In contrast, clouds analyzed around 75,000, 76,000, and 77,000 s UT have particle molar ratios larger than 4.5 and volumes less than 0.5 μm^3/cm^3 at temperatures 2 to 3 K above T_{ICE} (*26*), consistent with calculations for ternary solution droplets (*10, 12*). The persistence of NAT particles even at temperatures above the NAT equilibrium temperature [assuming 10 parts per billion by volume (ppbv) HNO_3 (*27*); see 77,700 and 78,400 s UT in Fig. 3], may indicate that evaporation of these particles occurs over several hours, which directly increases the time scales for chlorine processing during polar spring (*28*).

Antarctic polar stratospheric clouds are present throughout the winter and last well into spring when the large ozone losses occur. Because low temperatures prevail for long periods, the formation of NAT and ice particles is believed to dominate the particle composition. Meteorological conditions are substantially dif-

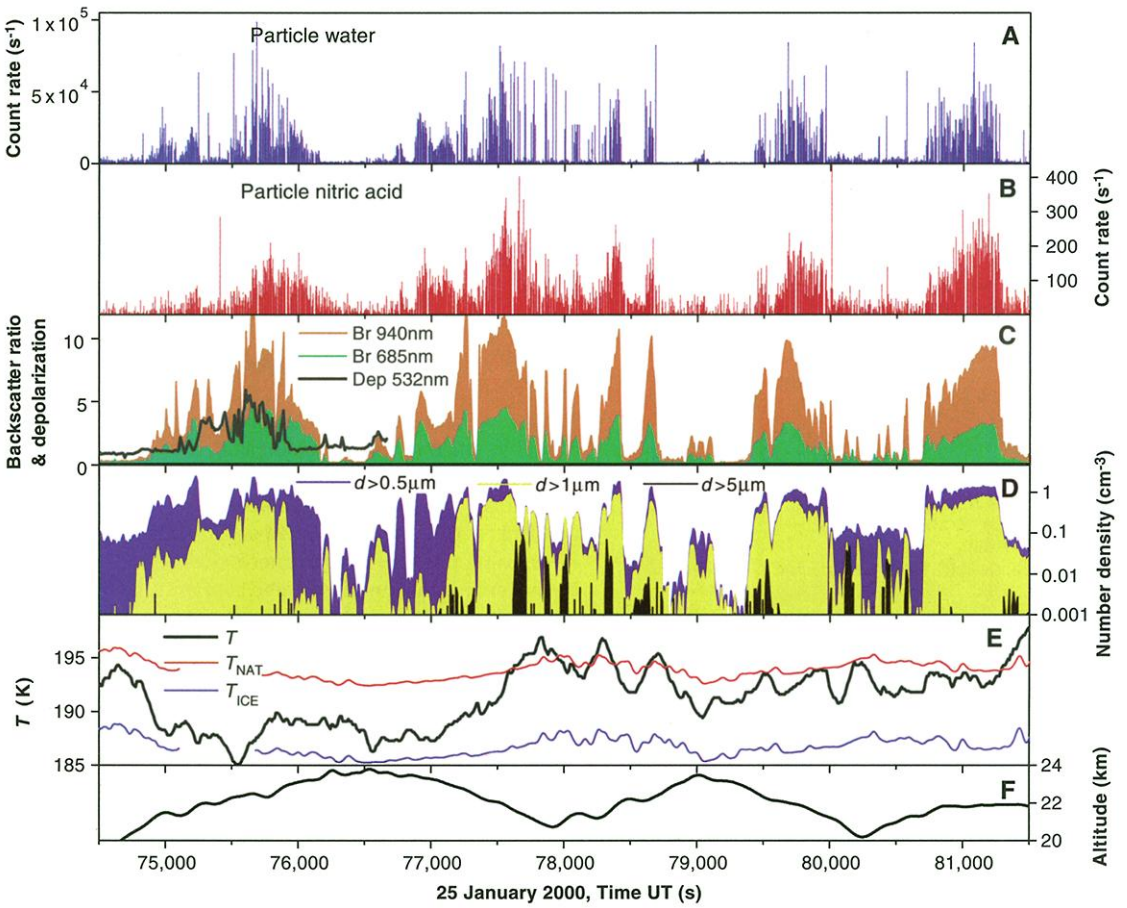

Fig. 2. Summary of the data obtained during the flight. (**A** and **B**) Condensed water and nitric acid ACMS data, measured at masses 18 and 63 amu, respectively. Each data point corresponds to particles contained in 3 cm^3 of air. (**C**) Backscatter ratio measurements at 940 and 685 nm. Backscatter sonde signals are excellent markers of the presence of clouds. The depolarization experiment provided data only during the first ascent (black line to 76,500 s). (**D**) Integrated number density of three selected particle size classes. A close correlation is found in PSCs among water and nitric acid count rates, backscatter ratios, and particle concentration. (**E**) The measured temperature (black line), the frost point temperature T_{ICE} derived from data of the water vapor experiment, and the calculated T_{NAT} temperature, assuming 10 ppbv HNO_3. (**F**) The altitude of the gondola.

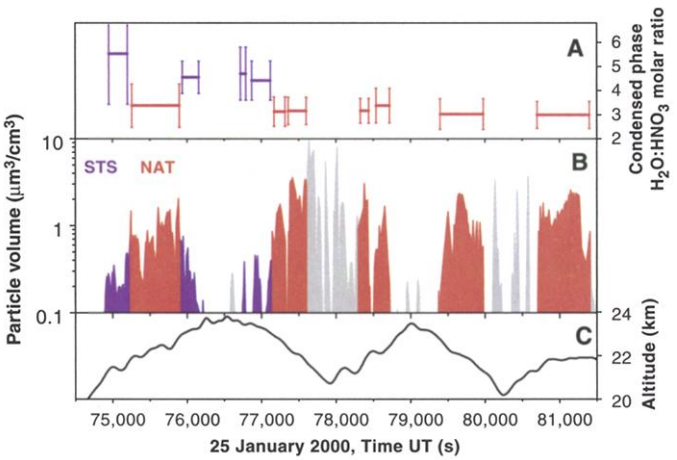

Fig. 3. Measured molar ratios (H_2O:HNO_3) of PSCs (**A**), together with the total particle volume in 1 cm^3 of air (**B**) and the altitude of the gondola (**C**) for reference. During the first ascent, the presence of STS particles is supported by low depolarization ratios (first and second blue areas, Fig. 2D) and of NAT particles by higher ratios near 75,500 s UT. During the periods marked as gray areas in (B), particles were detected by the ACMS; counting statistics, however, were not sufficient to derive molar ratios.

ferent in the north, where low-temperature periods are shorter and the vortex is less stable (*29, 30*). The question has been raised as to whether NAT particles can form in such an environment, although measurements have shown layers of liquid and solid aerosols at cold stratospheric temperatures (*31–33*). Our results confirm that NAT particles exist in the atmosphere and are present in the north polar stratosphere, near or even above their equilibrium temperature. The complexity of particle occurrence, phase, and composition in the northern polar region has been known for some time (*1, 34*). Two flights of the ACMS have confirmed the existence of non-ice PSC particles by measurements of STS droplets in low-temperature PSCs in January 1998 (*14*) and NAT particles at higher temperatures in January 2000.

References and Notes

1. World Meteorological Organization (WMO), *Scientific Assessment of Ozone Depletion: 1998, Report 44* (Global Ozone Research and Monitoring Project, Geneva, 1999).
2. S. Solomon, *Rev. Geophys.* **37**, 275 (1999).
3. S. Pawson, B. Naujokat, *J. Geophys. Res* **104**, 14209 (1999).
4. L. R. Poole, M. P. McCormick, *Geophys. Res. Lett.* **15**, 21 (1988).
5. L. R. Poole, M. T. Osborn, W. H. Hunt, *Geophys. Res. Lett.* **15**, 867 (1988).
6. D. Fahey *et al.*, *J. Geophys. Res.* **94**, 11299 (1989).
7. P. J. Crutzen, F. Arnold, *Nature* **324**, 651 (1986).
8. O. B. Toon, P. Hamill, R. P. Turco, J. Pinto, *Geophys. Res. Lett.* **13**, 1284 (1986).
9. D. R. Hanson, K. Mauersberger, *Geophys. Res. Lett.* **15**, 855 (1988).
10. A. Tabazadeh, R. P. Turco, M. Z. Jacobson, *J. Geophys. Res.* **99**, 12897 (1994).
11. G. Beyerle, R. Neuber, O. Schrems, F. Wittrock, B. Knudsen, *Geophys. Res. Lett.* **21**, 57 (1994).
12. K. S. Carslaw *et al.*, *Geophys. Res. Lett.* **21**, 2479 (1994).
13. L. Iraci, A. T. J. Fortin, M. A. Tolbert, *J. Geophys. Res.* **103**, 8491 (1998).
14. J. Schreiner, C. Voigt, K. Mauersberger, F. Arnold, N. Larsen, *Science* **283**, 968 (1999).
15. N. Larsen *et al.*, *J. Geophys. Res.* **105**, 1491 (2000).
16. C. Voigt *et al.*, *Geophys. Res. Lett.*, in press.
17. J. Schreiner, U. Schild, C. Voigt, K. Mauersberger, *Aerosol Sci. Technol.* **31**, 373 (1999).
18. D. J. Hofmann, T. Deshler, *J. Geophys. Res.* **96**, 2897 (1991).
19. T. Deshler, S. J. Oltmans, *J. Atmos. Chem.* **30**, 11 (1998).
20. J. M. Rosen, N. T. Kjome, *Appl. Opt.* **30**, 1552 (1991).
21. A. Adriani *et al.*, in *Proceedings of XVIII Quadrennial Ozone Symposium, L'Aquila 1996, Atmospheric Ozone*, R. D. Bojkov, G. Visconti, Eds. (Edigrafital for Parco Scientifico e Tecnologico d'Abruzzo, L'Aquila, Italy, 1998), vol. 2, pp. 879–882.
22. J. Ovarlez, H. Ovarlez, *Geophys. Res. Lett.* **21**, 13, 1235 (1994).
23. A. Dörnbrack, M. Leutbecher, R. Kivi, E. Kyrö, *Tellus* **51A**, 951 (1999).
24. The mass spectrometer sensitivities for water and nitric acid have been calibrated through the introduction of known partial pressures of these substances into the particle evaporation sphere by means of a pressure-related dynamic expansion. The mole flux to the mass spectrometer can then be related to the count rate.
25. The selection of the integration period was guided by the measurements of the backscatter sondes and by the mass spectrometer signals of H_2O and HNO_3 (Fig. 2). The actual period selected for the integration is not very critical; for example, integration in a cloud layer for 100 s did not change the molar ratio beyond the uncertainties shown in Fig. 3. The beginning and the end of a cloud encounter were always well resolved.
26. The total particle volume was calculated from a bimodal log-normal fit to the particle size distribution measured with the particle counter. STS particles (e.g., centered around 75,100 s UT) resulted in distributions of particles with a median diameter of 0.14 μm (standard deviation σ = 1.85) and a number density of 15 cm^{-3} and, for the second mode, in diameters of 1.08 μm (σ = 1.55) and number density of 0.01 cm^{-3}. NAT particles (e.g., near 79,650 s UT) resulted in a median diameter of 0.13 μm (σ = 1.50) and a density of 16 cm^{-3} and in a diameter of 1.52 μm (σ = 1.45) and a density of 0.5 cm^{-3}.
27. Although no direct HNO_3 gas phase measurement was performed, a mixing ratio of 10 ppb is reasonable [S. Spreng, F. Arnold, *Geophys. Res. Lett.* **21**, 1251 (1994)]. Departures of 2.5 ppb will change T_{NAT} by less than 0.5 K.
28. One of us (N.L.) calculated the evaporation times of NAT particles assuming a 1 K temperature increase: The time for a 50% volume reduction is 2 hours for a particle of radius 1.0 μm, and 1 day for a particle of radius 5.0 μm.
29. R. Stolarski, *Nature* **389**, 788 (1997).
30. P. A. Newman, J. G. Gleason, R. D. McPeters, R. S. Solarski, *Geophys. Res. Lett.* **24**, 2689 (1997).
31. K. S. Carslaw *et al.*, *Nature* **391**, 675 (1998).
32. K. S. Carslaw *et al.*, *J. Geophys. Res.* **103**, 5785 (1998).
33. T. Deshler *et al.*, *J. Geophys. Res.* **105**, 3943 (2000).
34. T. Peter, *Annu. Rev. Phys. Chem.* **48**, 785 (1997).

35. The balloon flight was performed as part of the European-American THESEO-2000/SOLVE campaign in winter 1999/2000. The excellent support through the balloon launch team of the Centre National d'Etudes Spatiales (CNES) is acknowledged. Supported by the Commission of the European Union through the Environmental and Climate program (contract ENV4-CT97-0523) and by NSF grants OPP-9707520 and OPP-9423285 (T.D., C.K., and J.R.).

24 August 2000; accepted 26 October 2000

Reinterpreting Space, Time Lags, and Functional Responses in Ecological Models

Matt J. Keeling,[1]* Howard B. Wilson,[2] Steve W. Pacala[3]

Natural enemy-victim interactions are of major applied importance and of fundamental interest to ecologists. A key question is what stabilizes these interactions, allowing the long-term coexistence of the two species. Three main theoretical explanations have been proposed: behavioral responses, time-dependent factors such as delayed density dependence, and spatial heterogeneity. Here, using the powerful moment-closure technique, we show a fundamental equivalence between these three elements. Limited movement by organisms is a ubiquitous feature of ecological systems, allowing spatial structure to develop; we show that the effects of this can be naturally described in terms of time lags or within-generation functional responses.

Enemy-victim systems incorporate a large cross section of ecological interactions, including predator-prey, host-parasitoid, host-parasite, and host-pathogen systems. A number of important questions about these systems have emerged from both theoretical and empirical work over many decades. For example, given the inherent instabilities in the dynamics of such interactions, how do the species coexist? How do density dependence and the behavioral responses of the organisms influence the dynamics? What are the effects of limited movement in space, leading to noncomplete mixing? A unifying explanation or approach has re-